http://www.geojournals.cn/dzxbcn/ch/index.aspx

# $^{40}Ar/^{39}Ar$ Dating of Deformation Events and Reconstruction of Exhumation of Ultrahigh-Pressure Metamorphic Rocks in Donghai, East China

LI Jinyi, YANG Tiannan, CHEN Wen and ZHANG Sihong
*Institute of Geology, Chinese Academy of Geological Sciences, Beijing 100037*
*E-mail: jyli@cags.net.cn*

**Abstract** Recent investigations reveal that the ultrahigh-pressure metamorphic (UHPM) rocks in the Donghai region of East China underwent ductile and transitional ductile-brittle structural events during their exhumation. The earlier ductile deformation took place under the condition of amphibolite facies and the later transitional ductile-brittle deformation under the condition of greenschist facies. The hanging walls moved southeastward during both of these two events. The $^{40}Ar/^{39}Ar$ dating of muscovites from muscovite-plagioclase schists in the Haizhou phosphorous mine, which are structurally overlain by UHPM rocks, yields a plateau age of 218.0±2.9 Ma and isochron age of 219.8Ma, indicating that the earlier event of the ampibolite-facies deformation probably took place about 220 Ma ago. The $^{40}Ar/^{39}Ar$ dating of oriented amphiboles parallel to the movement direction of the hanging wall on a decollement plane yields a plateau age of 213.1±0.3 Ma and isochron age of 213.4±4.1 Ma, probably representing the age of the later event. The dating of pegmatitic biotites and K-feldspars near the decollement plane from the eastern Fangshan area yield plateau ages of 203.4±0.3 Ma, 203.6±0.4 Ma and 204.8±2.2 Ma, and isochron ages of 204.0±2.0 Ma, 200.6±3.1 Ma and 204.0±5.0 Ma, respectively, implying that the rocks in the studied area had not been cooled down to closing temperature of the dated biotites and K-feldspars until the beginning of the Jurassic (about 204 Ma). The integration of these data with previous chronological ages on the ultrahigh-pressure metamorphism lead to a new inference on the exhumation of the UHPM rocks. The UHPM rocks in the area were exhumed at the rate of 3–4 km/Ma from the mantle (about 80–100 km below the earth's surface at about 240 Ma) to the lower crust (at the depth of about 20–30km at 220 Ma), and at the rate of 1–2 km/Ma to the middle crust (at the depth of about 15 km at 213 Ma), and then at the rate of less than 1 km/Ma to the upper crust about 10 km deep at about 204 Ma.

**Key words:** ultrahigh-pressure metamorphic rocks, structural deformation, $^{40}Ar/^{39}Ar$ dating, exhumation, Donghai, East China

## 1 Introduction

Since coesite and diamond inclusions were discovered in eclogites and their county rocks in the Dabie and Su-Lu areas (Xu, 1987; Okay et al., 1989; Hirajima et al., 1990; Enami and Zhang, 1990; Zhang et al., 1990; Xu et al., 1992; Wang and Liou, 1992; Masaki et al., 1993; Yang et al., 1993; Liou and Zhang, 1996; Wallis et al., 1997; Hu et al., 2001), the origin and exhumation of these rocks were discussed based on the analysis and investigation of regional geology, petrology, mineralogy, and metamorphic evolution (Chen et al., 1992; Li et al., 1995; Zhang Ru-yuan et al., 1995; Hacker et al., 1995; Liou et al., 1996) and various exhumation models were put forward (Wang et al., 1992; Okay et al., 1993; Platt, 1993; Ernst et al., 1994; Muruyama et al., 1994; Cong, 1994, 1996; Hacker et al., 1995; Liu et al., 1999, 2000; Cheng et al., 2000; Jian et al., 2000; Dong et al., 2002). However, these discussions and exhumation models are not constrained with structural geology and accurate chronological data.

It is well known the ultrahigh-pressure metamorphic (UHPM) rocks underwent multiple phases of thermal-dynamic tectonic events during their exhumation from the mantle to the earth's surface. Not only various coexisting mineral assemblages but also structural deformation features are formed in these events. Thus, an investigation into the structural deformation and thermal evolution of these rocks may constrain their exhumation from another side. In recent years, the authors investigated the structural deformation of the UHPM rocks in the Donghai region of the southern Sulu area, East China in carrying out the site selection of the first scientific drilling well of China and distinguished two phases of tectonic events in the process of the exhumation of the UHPM rocks, the earlier of which is characteristic of ductile deformation under the condition of amphibolite facies, and the latter of transitional ductile-brittle one under green-schist facies. $^{40}Ar/^{39}Ar$ dating of syn-tectonic metamorphic minerals indicates that these two events occurred in the Late Triassic. And then, the exhumation of the UHPM rocks from the mantle (eclogite facies) to the lower of the upper crust (greenschist facies) is primarily reconstructed on the basis of the integration of

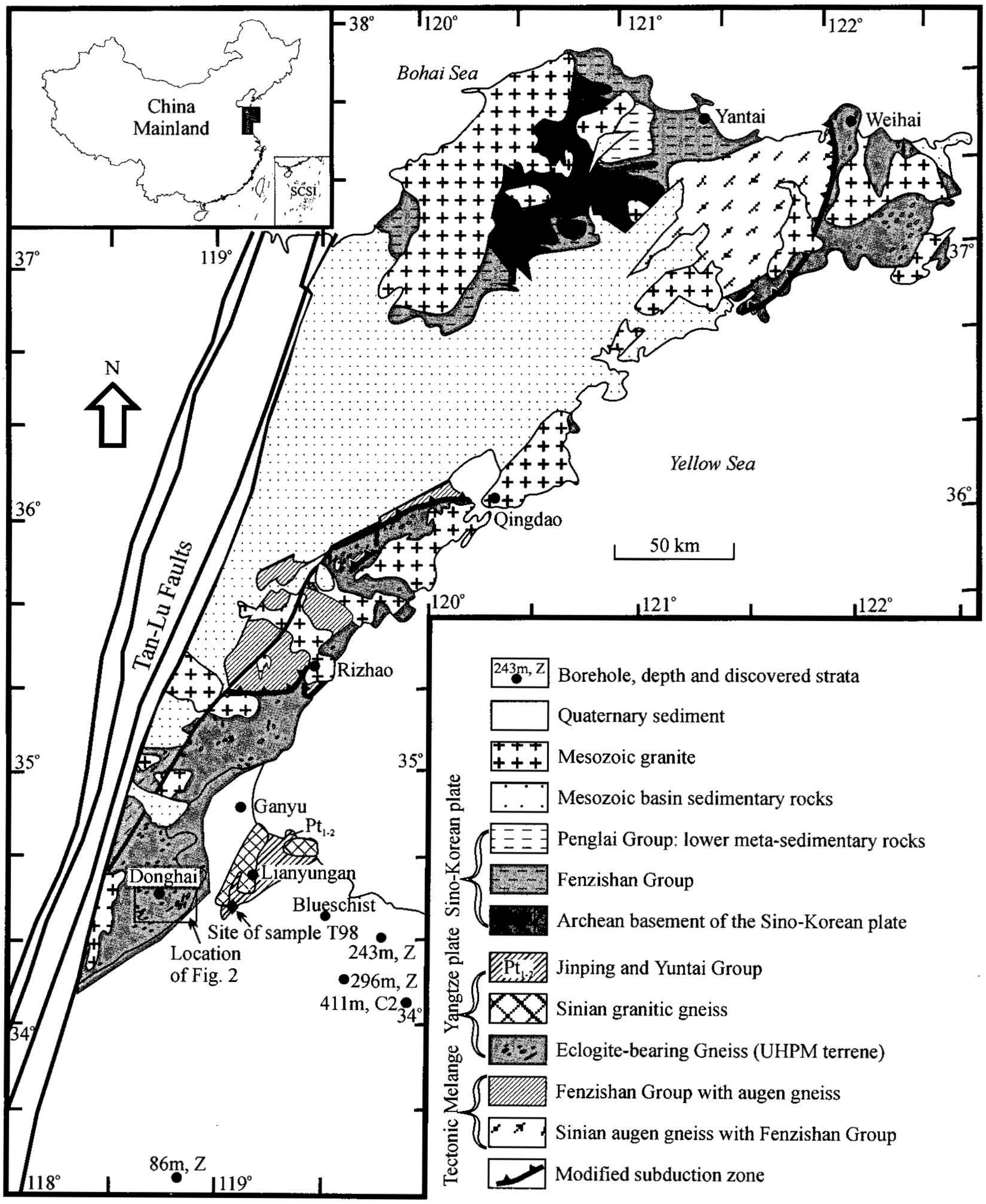


Fig. 1. Geological map of the Sulu UHPM terrane.

this study and previous investigations.

## 2 Regional Geology

The Sulu HPM (high-pressure metamorphic) -UHPM terrane of East China means the area of southern Shandong peninsula and northern Jiangsu plain east of the Tan-Lu sinistral strike-slip fault belt (Fig. 1) and is a part of the Triassic collision belt between the Yangtze and Sino-Korean blocks. The belt extended eastwards to the central Korean peninsula (Yin and Nie, 1993; Lee et al., 1997) and westwards through Dabieshan and Tongbaishan to Qinling (Zhang Guowei et al., 1995; Meng and Zhang, 1999).

The Sulu UHPM terrane is structurally a composite dome-like framework with a NE-extending long axis and intruded by Late Mesozoic granites, the center of the dome is located in the Taoyuan-Donglonggu region of the southern Shandong peninsula (Yang et al., 1996).

The Donghai region is located in the south of the Sulu HPM-UHPM terrane and consists mainly of felsic gneisses and minor eclogites and serpentinized garnet peridotites. Drilling data obtained by the local geological institutions suggest that there exist various tectonic units under the Quaternary sediments of the north Jiangsu plain. The units

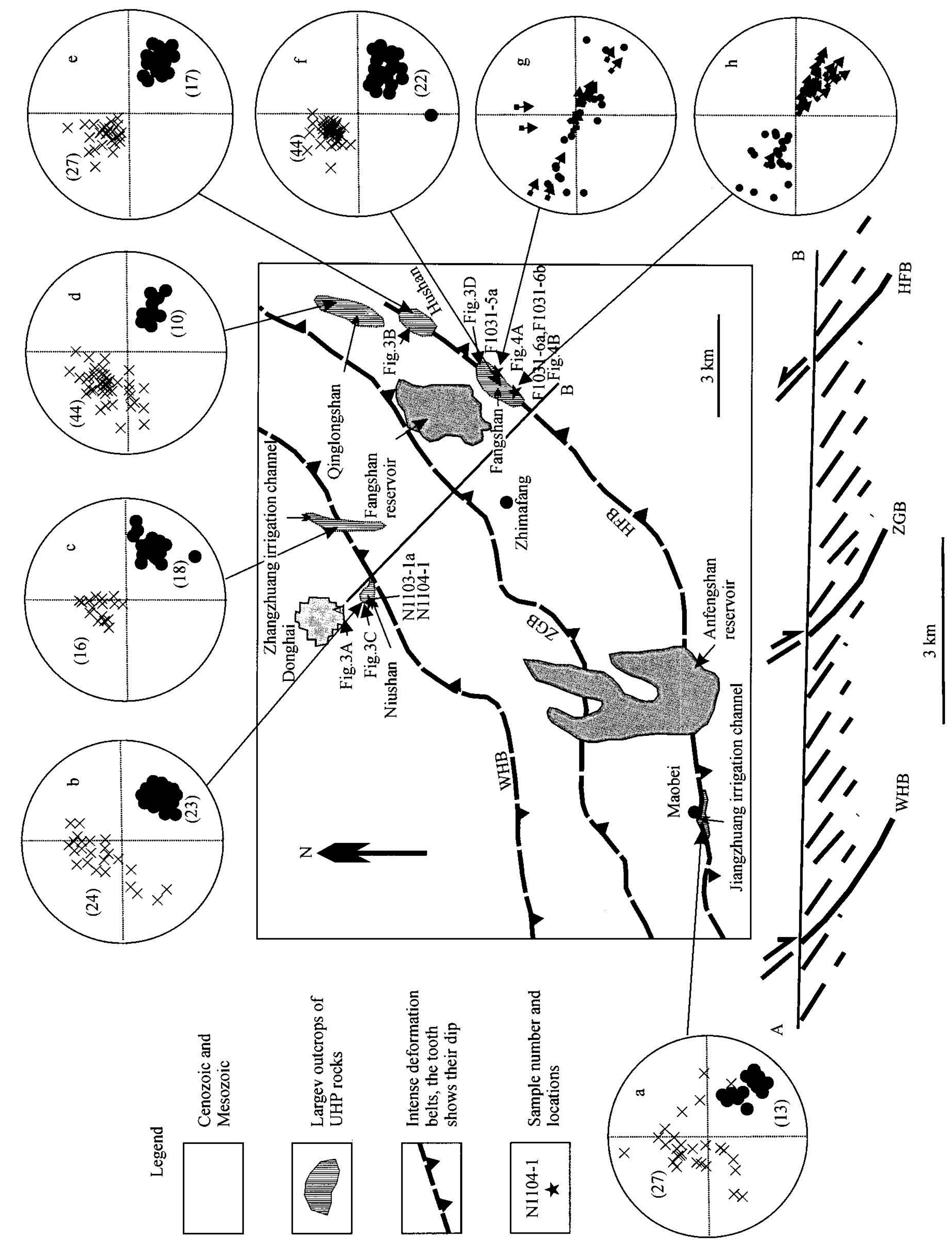


Fig. 2. Tectonic framework of the Donghai region.
a–h are stereographic projections on the lower hemisphere of poles of foliation (cross in a–f), stretching lineation (dot in a–f), poles of slipping planes (small dots in g and h), and striation lineation (black squares in g and h, arrows show the slipping direction). Numbers in parentheses on a–f are numbers of measured foliations and lineations. Locations of Fig. 3, Fig. 4 and sites of samples for $^{40}Ar/^{39}Ar$ dating are shown on this map. WHB – Wuzhuang-Houcaozhuang ductile shearing belt; ZGB – Zhimafang-Guodun ductile shearing belt; HFB – Hushan-Fangshan ductile shearing belt.

include, from north (upper) to south (lower), UHPM rocks, HPM rocks, Sinian-Paleozoic sedimentary cover, and Pre-Sinian metamorphic crystalline basement of the Yangtze block.

An analysis of the Sinian-Triassic sedimentary environments of the northern Yangtze passive margin indicates that the collisional orogeny between the Yangtze and Sino-Korean blocks took place in the middle of the Triassic (Li, 2001). The syn-collision deformation of the foreland fold-thrust belt in the middle-lower areas of the Yangtze River occurred at the end of the Triassic and is characteristic of south-verging thrust and overturn folds (Zhu et al., 1999). The deformation associated with the dome was formed in the Early Cretaceous. The north-

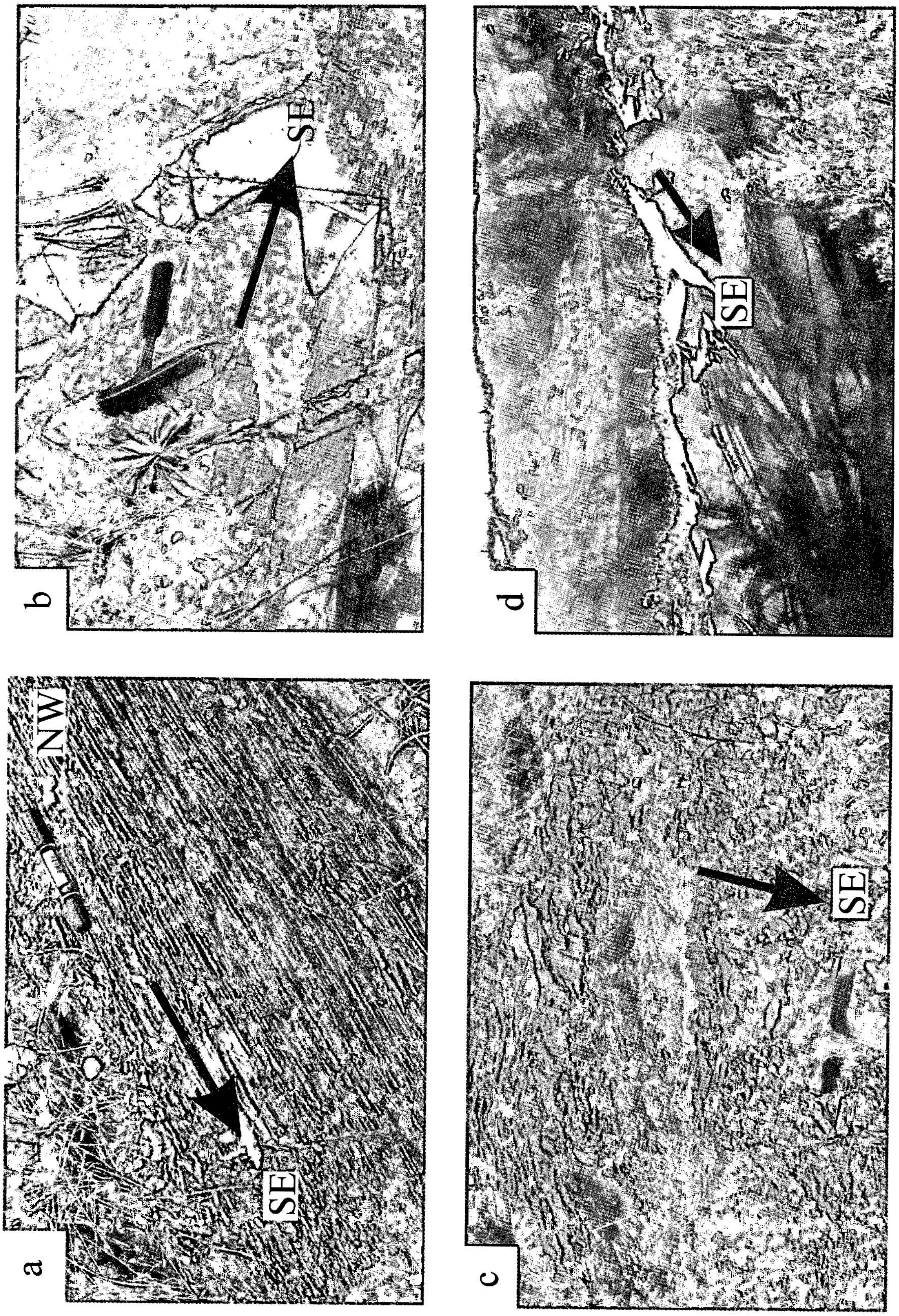


Fig. 3. Stretching lineation (Picture a from the southern suburb of Donghai town, arrow indicating dip of the lineation) and A-type folds (Picture b from Hushan, Picture c from Niushan, and Picture d from Fangshan; arrows showing the plunging of hinges) of the earlier ductile shearing deformation.

verging thrusts and folds of sedimentary strata in the foreland belt (Li, 1994) are probably the result of the indentation of the UHPM and HPM tectonic slices in the southern side of the dome southwards into the cover sequences of the northern Yangtze margin.

## 3 Structural Deformation of UHPM Rocks in the Donghai Region

Geographically, the Donghai region is part of the northern Jiangsu Quaternary plain. Outcrops of UHPM rocks in the region are visited only in some quarries in lower hills such as Niushan, Fangshan, Hushan, and Qinglongshan, in some artificial irrigation channels such as Jiangzhuang and Zhangzhuang, and in some pits for digging and mining crystals and vermiculite by local residents. The structural framework of the UHPM rocks of the region is described as alternating anticlinorium and synclinorium with NE-extending hinges by local geologists. However, our field observation of lineations, hinges of folds, rotational deformation of feldspar porphyroblasts and felsic veins, and S-C fabrics, revealed a more complicated tectonic configuration and evolution and two phases of pre-Cretaceous southeast-verging deformation events in the exhumation of the UHPM rocks, i.e. an earlier of ductile shearing deformation under the condition of amphibolite facies, and a later of transitional ductile-brittle decollement under the condition of green-schist facies.

### 3.1 Ductile Shearing Deformation

The ductile shearing deformation event is responsible for the occurrence of alternating narrow, intense shearing belts with a NE-SW strike and southeastward moderate dip and wide, weak deformational domains in the UHPM rocks of the region.

Three intense ductile shearing belts are distinguished as the Wuzhuang-Houcaozhuang (WHB), Zhimafang-Guodun (ZGB), and Hushan-Fangshan (HFB) belts (Fig. 2). In these belts, UHPM rocks are involved into A-type folds with southeast-plunging hinge and penetrative stretching lineations with similar attitudes (Fig. 3), and eclogites in pods in gneisses underwent retrograde metamorphism of amphibolite facies, were almost changed into amphibolites and stretched in the direction parallel to the strike of the hinges and lineations. The rotation of feldspar porphyries and S-C microfabrics in these rocks indicate that the shearing vector is dominated by the southeastward movements. The only S-C macrofabrics on the scale of outcrop indicating the opposite shearing vector is observed in one outcrop in Fangshan in the Hushan-Fangshan belt. Tow possible explanations for the rightabout shearing vectors in different deformation belts of the region are tentatively proposed. One is that the opposite vectors are the results of an extrusion deformation of the same phase in a closed system, and the other is that they are formed in different deformation events. The limited spatial distribution and non-penetrative deformation features of the northward shearing vector show that it occurred in the post-dome crustal shortening.

The weak deformation domains between the above intense shearing belts are characterized by non-penetrative stretching lineations and relatively broad A-type folds. So, fresh eclogites may be seen in these domains.

In one pit in the Haizhou phosphorous mining area near the southern suburb of Lianyungang, granite-gneisses similar to regional eclogite-trapping gneisses are thrust southwards onto a muscovite-plagioclase schist, in which there is only a mineral assemblage of muscovite-plagioclase-quartz, indicating its being the result of the amphibolite-facies metamorphism.

### 3.2 Transitional ductile-brittle deformation

In quarries in eastern Fangshan and western Niushan, southeast-dipping faults cutting the above intense shearing belts and regional foliation may be observed. In quarries in eastern Fangshan, the dip of later faults is mainly to southeast with dip angles ranging from less than 5° to 70°, and in some outcrops, the dip of one plane is changed from moderately northwards through sub-horizontal to moderately southeastwards, constituting a wavy, south-dipping fault plane. Amphiboles oriented in the directions of northwest to southeast occur on the planes. Striations and steps on the planes imply that the hanging wall of the faults slipped down southeastwards (Fig. 2g and h). Near the fault plane there occur pods and veins of pegmatite consisting of K-feldspars and biotites and no evidence of their being disturbed by structural deformation is observed (Fig. 4).

On the western slope of the Niushan Mnt., a southeast-dipping fault with a dip angle of 45° similar to the above one is observed. On the plane, oriented amphiboles occur.

The above phenomenon reveals that a deformation phase with transitional ductile-brittle features followed the earlier ductile shearing event. The growth of amphiboles on the fault planes and occurrence of pegmatite pods near the planes show that the later event may have taken place under the condition of greenschist-facies metamorphism with moderate activities of fluids.

## 4 $^{40}Ar/^{39}Ar$ Dating of Syn-deformational Metamorphic Minerals

### 4.1 Sample collecting and analytical method

Six samples for $^{40}Ar/^{39}Ar$ dating were collected from the Haizhou phosphorous mine, Niushan and Fangshan in order to determine the ages of the above two phases of deformation events.

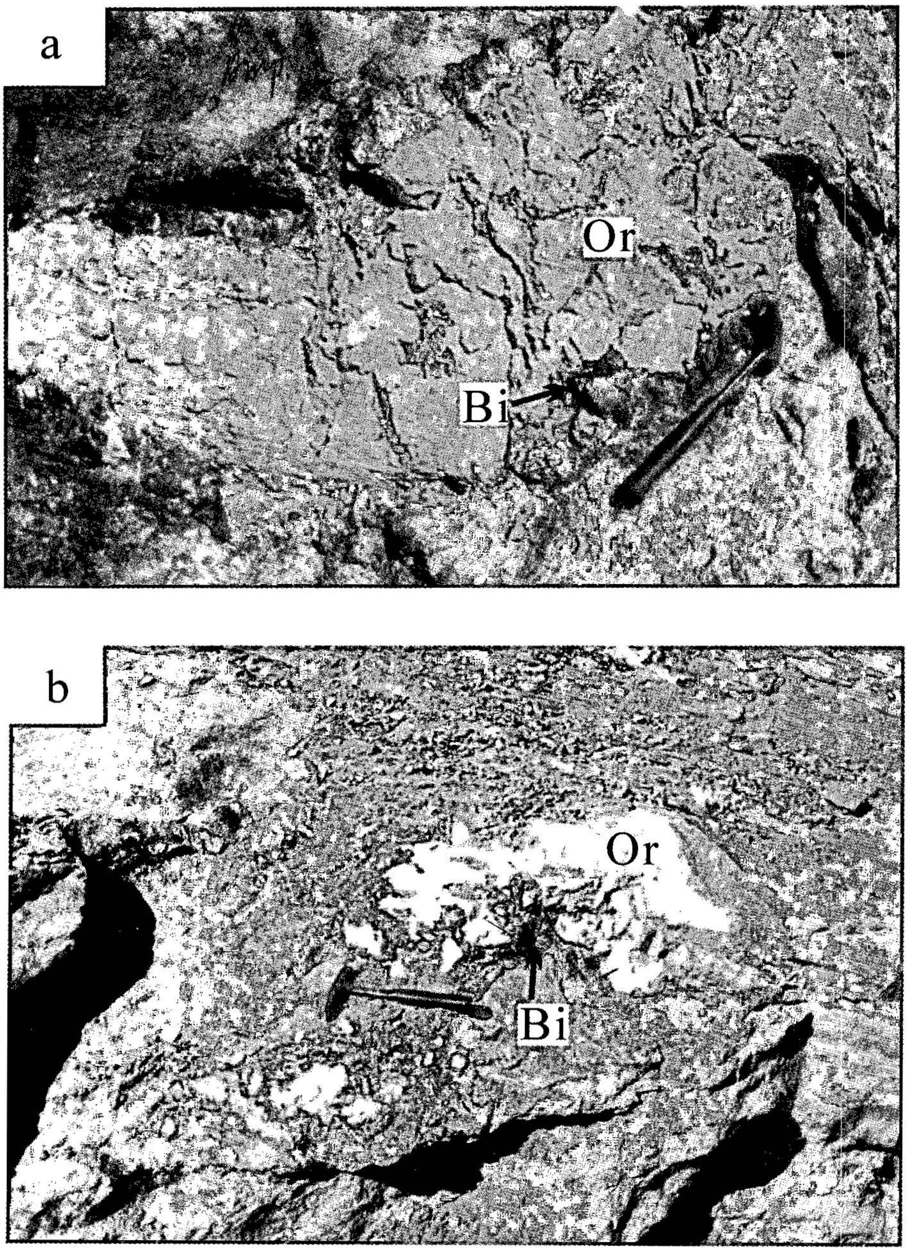


Fig. 4. K-feldspar-biotite pegmatite pods near the transitional brittle-ductile decollement fault in the Fangshan quarries.

One sample from the Haizhou mine was collected from muscovite-plagioclase schists in an exploration pit, which is located in the lower wall of the southeastward thrusting system on the southern margin of the mine. Muscovites (T98) were separated from the sample for $^{40}Ar/^{39}Ar$ dating.

Two samples from Niushan were collected from K-feldspar porphyroblasts with southeast-verging rotating deformation in felsic gneisses, which were involved into the penetrative ductile shearing deformation, and from oriented amphiboles on the fault planes with the hanging wall slipping down southeastwards. The K-feldspar (N1103-1a) and amphibole (N1104-1) for $^{40}Ar/^{39}Ar$ dating were separated from these two samples, respectively.

Three samples from the eastern Fangshan quarries, F1031-5 (biotite) from a northern pit of the Qianyangzhuang quarry, F1031-6a (biotite) and F1031-6b (K-feldspar) from the Shanqian quarry were collected from pods of pegmatite near a fault plane in the lower wall of a southeastward down-slipping decollement fault. The pegmatites are mainly composed of K-feldspar, and minor biotites are trapped in the interior of and/or occur on the margin of these pegmatites. No evidence shows that there are later tectono-thermal events in these sites.

The monomineral grains for $^{40}Ar/^{39}Ar$ dating from these six samples were purified using Magnetic Separator and then were cleaned with ultrasonic treatment in ethanol, making their purity more than 99%. The purified samples were respectively irradiated for 55 hours in the nuclear reactor of the Chinese Institute of Atomic Energy, Beijing. And then, the Ar isotopic ratios of the irradiated samples were analyzed by the MM-1200 Mass Spectrometer of the Institute of Geology, Chinese Academy of Geological Sciences, Beijing, and Institute of Geology of the China Seismological Bureau, Beijing. The above procedures have been described in detail by Fu et al. (1987). The reactor delivers a neutron flux of about $7.6\times10^{12}$ n $cm^{-2}s^{-1}$, and its integrated neutron flux of about $1.5\times10^{18}$ n $cm^{-2}$ during the irradiating processes. All the measured data were corrected for mass discriminations, atmospheric Ar component, blanks and irradiation-induced mass interference. The correction factors of interfering isotopes produced during the irradiation were determined by the analyses of

**Table 1 Stepwide heating results of $^{40}Ar/^{39}Ar$ dating for muscovite (T98) from the Haizhou phosphorous mine***
Sample weight: 53.40 mg, j=0.002265

| Temperature (°C) | $(^{40}Ar/^{39}Ar)_m$ | $(^{36}Ar/^{39}Ar)_m$ ($10^{-3}$) | $(^{37}Ar/^{39}Ar)_m$ | $(^{40}Ar/^{39}Ar)^*$ | $^{39}Ar$ ($10^{-12}$ mol) | $^{39}Ar$ release cumulate (%) | ages (Ma) |
|---|---|---|---|---|---|---|---|
| 600 | 156.6 | 0.0000 | 1.058 | 157.2 | 0.000 | 0.013 | 549.4±6.7 |
| 700 | 66.36 | 0.0000 | 0.0714 | 66.38 | 0.003 | 0.203 | 252.7±3.3 |
| 750 | 64.57 | 13.55 | 0.0096 | 60.56 | 0.025 | 1.62 | 231.9±3.3 |
| 800 | 58.14 | 2.441 | 0.0015 | 57.42 | 0.157 | 10.5 | 220.6±3.0 |
| 830 | 57.49 | 1.550 | 0.0009 | 57.03 | 0.278 | 26.3 | 219.2±2.9 |
| 850 | 57.19 | 0.3954 | 0.0006 | 57.06 | 0.384 | 48.0 | 219.3±2.9 |
| 870 | 57.04 | 1.495 | 0.0010 | 56.60 | 0.254 | 62.4 | 217.6±2.9 |
| 900 | 57.16 | 1.909 | 0.0013 | 56.59 | 0.193 | 73.3 | 217.6±2.9 |
| 920 | 57.16 | 3.117 | 0.0024 | 56.24 | 0.101 | 79.1 | 216.3±2.9 |
| 950 | 57.17 | 2.175 | 0.0019 | 56.52 | 0.132 | 86.6 | 217.3±2.9 |
| 1000 | 56.82 | 2.360 | 0.0026 | 56.12 | 0.095 | 91.9 | 215.9±2.9 |
| 1030 | 56.32 | 2.250 | 0.0023 | 55.65 | 0.105 | 97.9 | 214.2±2.9 |
| 1150 | 56.44 | 2.514 | 0.0081 | 55.69 | 0.030 | 99.6 | 214.3±2.9 |
| 1200 | 62.53 | 35.52 | 0.8265 | 52.12 | 0.005 | 99.8 | 201.3±3.3 |
| 1320 | 69.22 | 44.88 | 0.2633 | 55.99 | 0.003 | 100 | 215.4±3.6 |

* Analyzed by Wang Yu in the Isotopic Laboratory of the Institute of Geology of the China Seismological Bureau.

irradiated pure salts of $K_2SO_4$ and $CaF_4$ and their values are: $(^{36}Ar/^{37}Ar)_{Ca}$=0.000240; $(^{40}Ar/^{39}Ar)_k$=0.004782; $(^{39}Ar/^{37}Ar)_{Ca}$=0.000806. The decay constant used is $\lambda=5.543\times10^{-11}a^{-1}$. All $^{37}Ar$ were corrected for radiogenic decay (half life of 35.1 days). The errors are 2σ deviations and correspond to the 95% confidence level. The standard monitor sample is a ZBH-25 biotite from a granodiorite in the West Hills of Beijing, with a $K_2O$ content of 7.6% and age of 133.5 Ma.

## 4.2 Analytical results and their geological implicatioms

The analytical results of the six samples are listed in Table 1 and Table 2, and shown in Fig. 5, Fig. 6 and Fig. 7.

Muscovites of sample T98 from muscovite-plagioclase schists in the Haizhou phosphorous mine yield a flat age spectrum with a plateau age of 218.0 ±2.9 Ma and isochron age of 219.8 Ma (see Table 1 and Fig. 5). No evidence for multi-stage metamorphism and single-age plateau of the sample indicate that the age of 218 Ma of the muscovite represents its cooling age. The K-Ar isotopic cooling temperature of muscovites is considered as ranging from 400–500°C (Dodson, 1973; McGrew and Snee, 1994; Lister and Baldwin, 1996), which is close to the minimum of the temperature range of amphibolite-facies metamorphism. Thus, the above cooling ages of T98 muscovites may be considered as representative of the minimum age of the metamorphism.

The dating results of two samples from Niushan are listed in Table 2 and shown in Fig. 6. An amphibole sample (N1104-1) of them yields a nearly flat age spectrum with the main plateau age of 213.3±0.3 Ma ($^{39}Ar$ cumulative of 89.4% in seven heating steps from 700°C–1100°C) and isochron age of 213.4± 4.1 Ma (Fig. 6), indicating that the K-Ar isotope system of the amphibole was closed at about 213 Ma and after that, is not disturbed by any other tectono-thermal events. Based on a higher closure temperature of the K-Ar isotopic system of amphibole (Dodson, 1973; McGrew and Snee, 1994; Lister and Baldwin, 1996), we consider that the cooling age of the above amphibole (N1104-1) represents the peak age of the transitional ductile-brittle deformational event. A K-feldspar sample (N1103-1a) yields a basically flat age spectrum (Fig. 6), and its total age is 191.3±2.1 Ma with a relevant isochron age of 190.3 ±3.1 Ma. The K-feldspar sample must have not been disturbed by the later transitional ductile-brittle event because its sampling site is located in a ductile shearing gneiss about 500 m away from the decollement plane. So, the age of about 190 Ma is probably representative of the cooling age of the K-feldspar sample. In other word, this means that the gneisses including the dated K-feldspar sample were not cooled down to the closing temperature of the K-Ar isotopic system of the K-feldspar until about 190 Ma.

The dating results of three samples from southeastern Fangshan are listed in Table 2 and shown in Fig. 7. Biotites of samples F1031-5 and F1031-6b yield $^{40}Ar/^{39}Ar$ flat age spectrums with plateau ages of 203.4±0.3 Ma and 203.6±0.4 Ma, and isochron ages of 204.0±2.0 Ma and 200.6±3.1 Ma (Fig. 7), possibly representing their cooling age. The $^{40}Ar/^{39}Ar$ age spectrum of sample F1031-6b K-feldspar shows a step-like age spectrum with a high plateau age of 212.7±0.7 Ma at two heating steps of 1125°C and 1220°C with $^{39}Ar$ release accumulate of 42.02%, which is basically the same as the age of the amphibole from Niushan and is probably closer to the peak age of later deformation event. The total and isochron ages of the sample are 204.8±2.2 Ma and 204.0±5.0 Ma (Fig. 7), respectively, similar to the above biotite ages and probably

**Table 2 Stepwide heating results of $^{40}Ar/^{39}Ar$ dating for amphibole, biotite and K-feldspar from Niushan and Fangshan of the Donghai region***

| Temperature (°C) | $(^{40}Ar/^{39}Ar)_m$ | $(^{36}Ar/^{39}Ar)_m$ | $(^{37}Ar/^{39}Ar)_m$ | $(^{40}Ar/^{39}Ar)^*$ | $^{39}Ar$ ($10^{-14}$ mol) | $^{39}Ar$ cumulate (%) | ages (Ma) |
|---|---|---|---|---|---|---|---|
| Amphibole from Niushan (N1104-1) sample weight: 280.0 mg, J=0.01678 | | | | | | | |
| 500 | 23.5398 | 0.0593 | 0.8773 | 6.0800 | 113.00 | 2.74 | 175.3±24.7 |
| 610 | 8.2470 | 0.0059 | 1.0998 | 6.5775 | 135.20 | 6.01 | 188.9±3.4 |
| 700 | 7.8374 | 0.0017 | 0.9948 | 7.3978 | 578.00 | 20.02 | 211.1±2.3 |
| 780 | 8.3925 | 0.0033 | 0.9934 | 7.4770 | 479.00 | 31.62 | 213.2±2.6 |
| 860 | 8.3132 | 0.0029 | 1.0920 | 7.5278 | 581.00 | 45.70 | 214.6±2.5 |
| 930 | 7.7778 | 0.0007 | 0.8893 | 7.6455 | 603.00 | 60.30 | 217.8±2.3 |
| 990 | 7.7069 | 0.0012 | 1.4402 | 7.4562 | 580.00 | 74.36 | 212.7±2.2 |
| 1050 | 7.5873 | 0.0005 | 1.0640 | 7.5237 | 630.00 | 89.62 | 214.5±2.2 |
| 1100 | 7.8661 | 0.0017 | 1.0787 | 7.4497 | 239.00 | 95.41 | 212.5±2.3 |
| 1185 | 7.9750 | 0.0029 | 0.9453 | 7.1808 | 120.00 | 98.32 | 205.2±2.4 |
| 1265 | 12.1053 | 0.0217 | 2.6051 | 5.8934 | 32.30 | 99.10 | 170.1±9.3 |
| 1400 | 12.9032 | 0.0134 | 2.5447 | 9.1527 | 37.20 | 100.00 | 257.0±6.2 |
| K-feldspar from Niushan (N1103-1a) sample weight: 118.1 mg, J=0.01678 | | | | | | | |
| 400 | 7.2698 | 0.0019 | 0.0123 | 6.7023 | 1835.00 | 13.97 | 192.3±2.4 |
| 500 | 6.6667 | 0.0007 | 0.0436 | 6.4511 | 690.00 | 19.22 | 185.4±2.2 |
| 610 | 6.6875 | 0.0006 | 0.0376 | 6.5009 | 800.00 | 25.32 | 186.8±2.0 |
| 700 | 6.7891 | 0.0008 | 0.0360 | 6.5511 | 626.00 | 30.08 | 188.1±2.0 |
| 780 | 6.8157 | 0.0011 | 0.1241 | 6.4952 | 364.00 | 32.85 | 186.6±2.0 |
| 860 | 6.8614 | 0.0011 | 0.0502 | 6.5378 | 458.00 | 36.34 | 187.8±2.0 |
| 930 | 6.8834 | 0.0012 | 0.0543 | 6.5425 | 564.00 | 40.63 | 187.9±2.0 |
| 1010 | 6.8873 | 0.0008 | 0.0206 | 6.6462 | 1118.00 | 49.15 | 190.7±2.0 |
| 1070 | 6.9048 | 0.0005 | 0.0285 | 6.7483 | 1344.00 | 59.38 | 193.5±2.0 |
| 1125 | 6.9177 | 0.0006 | 0.0135 | 6.7401 | 1700.00 | 72.32 | 193.3±2.0 |
| 1185 | 6.9377 | 0.0007 | 0.0135 | 6.7295 | 1156.00 | 81.13 | 193.0±2.0 |
| 1235 | 7.0118 | 0.0008 | 0.0184 | 6.7720 | 2125.00 | 97.30 | 194.2±2.0 |
| 1300 | 7.2993 | 0.0018 | 0.1370 | 6.7873 | 343.00 | 99.92 | 194.6±2.4 |
| 1400 | 11.8182 | 0.0364 | 2.1333 | 1.2212 | 11.00 | 100.00 | 36.6±16.2 |
| Biotite from Fangshan (F1031-5a) sample weight: 124.8 mg, J=0.01678 | | | | | | | |
| 400 | 8.9335 | 0.0064 | 0.0183 | 7.0485 | 3235.00 | 30.14 | 201.7±3.6 |
| 500 | 10.4038 | 0.0110 | 0.0116 | 7.1495 | 2600.00 | 54.36 | 204.4±5.0 |
| 610 | 8.4028 | 0.0042 | 0.0525 | 7.1708 | 576.00 | 59.73 | 205.0±2.7 |
| 700 | 7.8364 | 0.0024 | 0.0000 | 7.1331 | 1100.00 | 69.98 | 204.0±2.3 |
| 780 | 7.5511 | 0.0016 | 0.0151 | 7.0906 | 2005.00 | 88.66 | 202.8±2.2 |
| 860 | 7.6278 | 0.0020 | 0.0309 | 7.0211 | 978.00 | 97.77 | 200.9±2.3 |
| 930 | 9.1914 | 0.0070 | 0.1631 | 7.1282 | 186.00 | 99.50 | 203.8±3.6 |
| 1025 | 26.0000 | 0.0640 | 0.0000 | 7.0832 | 25.00 | 99.73 | 202.6±6.0 |
| 1140 | 26.8333 | 0.0667 | 0.0000 | 7.1286 | 12.00 | 99.84 | 203.8±6.1 |
| 1250 | 9.8214 | 0.0089 | 0.0000 | 7.1783 | 11.00 | 99.94 | 205.2±2.1 |
| 1300 | 54.9020 | 0.1569 | 6.0511 | 9.0170 | 5.00 | 99.99 | 254.2±61.4 |
| 1400 | 157.1429 | 0.5000 | 13.2260 | 10.4365 | 1.00 | 100.00 | 291.1±114.4 |
| Biotite from Fangshan (N1031-6a) sample weight: 70.6 mg, J=0.01678 | | | | | | | |
| 400 | 10.9649 | 0.0149 | 0.0616 | 6.5582 | 342.00 | 6.14 | 188.3±6.6 |
| 500 | 8.5114 | 0.0047 | 0.0335 | 7.1182 | 786.00 | 20.26 | 203.6±2.9 |
| 610 | 7.9110 | 0.0026 | 0.0255 | 7.1366 | 1034.00 | 38.84 | 204.1±2.4 |
| 700 | 8.5661 | 0.0045 | 0.0657 | 7.2399 | 401.00 | 46.04 | 206.8±2.8 |
| 810 | 7.9115 | 0.0028 | 0.1119 | 7.0785 | 1130.00 | 66.34 | 202.5±2.4 |
| 910 | 7.8717 | 0.0027 | 0.1977 | 7.0959 | 1278.00 | 89.30 | 202.9±2.4 |
| 990 | 8.0901 | 0.0034 | 0.1453 | 7.0848 | 555.00 | 99.27 | 202.7±2.5 |
| 1070 | 23.5918 | 0.0449 | 6.8016 | 10.8612 | 25.00 | 99.71 | 302.0±17.4 |
| 1235 | 48.3740 | 0.1626 | 24.0368 | 2.0637 | 12.30 | 99.93 | 61.4±71.4 |
| 1350 | 262.0000 | 0.8500 | 0.0000 | 10.8202 | 2.00 | 99.96 | 301.0±65.4 |
| 1400 | 135.0000 | 0.4000 | 0.0000 | 135.0000 | 2.00 | 100.00 | 448.0±28.7 |
| K-feldspar from Fangshan (F1031-6b) sample weight: 143.6 mg, J=0.01678 | | | | | | | |
| 400 | 7.4777 | 0.0018 | 0.0387 | 6.9350 | 2240.00 | 6.27 | 198.6±2.5 |
| 500 | 7.1633 | 0.0009 | 0.0108 | 6.8969 | 3490.00 | 16.05 | 197.6±2.1 |
| 610 | 7.0139 | 0.0008 | 0.0104 | 6.7643 | 1805.00 | 21.11 | 194.0±2.0 |
| 720 | 7.2998 | 0.0012 | 0.0090 | 6.9414 | 2085.00 | 26.95 | 198.8±2.1 |
| 830 | 7.1584 | 0.0013 | 0.0093 | 6.7594 | 2020.00 | 32.61 | 193.8±2.1 |
| 930 | 7.3266 | 0.0010 | 0.0054 | 7.0233 | 3460.00 | 42.30 | 200.9±2.1 |
| 1025 | 7.4011 | 0.0009 | 0.0009 | 7.1460 | 3540.00 | 52.21 | 204.3±2.1 |
| 1125 | 7.5681 | 0.0005 | 0.0010 | 7.4239 | 11020.00 | 83.08 | 211.8±2.2 |
| 1220 | 7.7889 | 0.0010 | 0.0008 | 7.4872 | 3980.00 | 94.23 | 213.5±2.2 |
| 1300 | 7.7885 | 0.0020 | 0.0148 | 7.1809 | 1272.00 | 97.79 | 205.2±2.3 |
| 1400 | 7.7893 | 0.0028 | 0.0717 | 6.9650 | 788.00 | 100.00 | 199.4±2.4 |

* Analyzed by Chen Wen and Zhang Sihong in the Isotopic Laboratory of the Institute of Geology of the Chinese Academy of Geological Sciences.

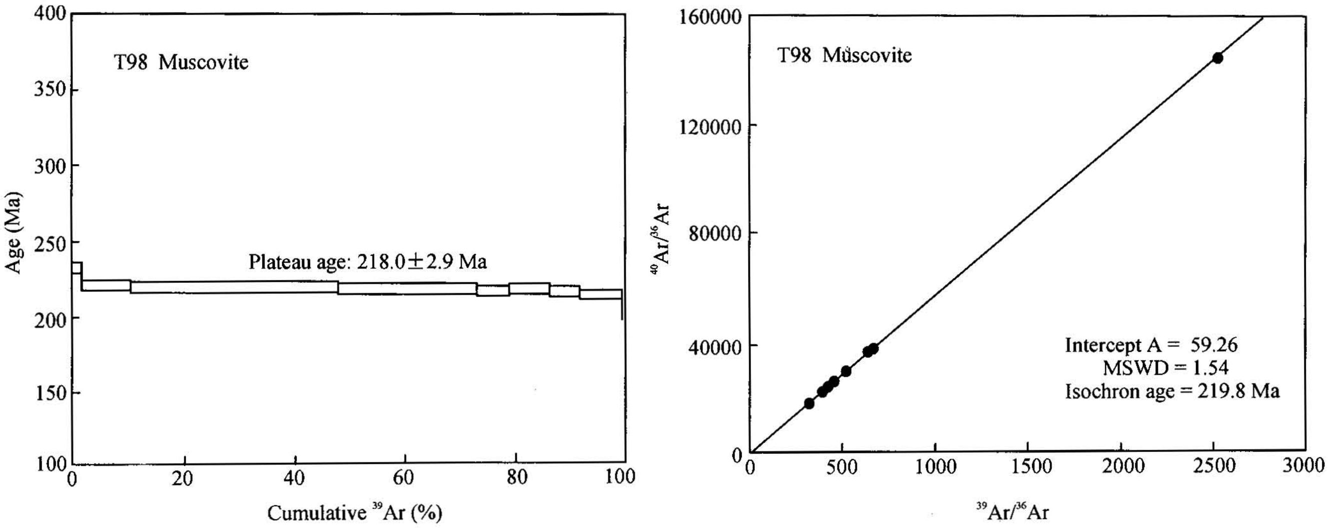


Fig. 5. $^{40}$Ar/$^{39}$Ar age plateau spectrum and isochron of Sample T98 muscovite from the Haizhou phosphorous mine.

representative of its cooling age.

## 5 Discussions

Generally, $^{40}$Ar/$^{39}$Ar ages of monominerals represent the K-Ar isotopic closing ages of the samples, and are younger than the crystallizing ages of these minerals. However, the difference between the closing and crystallizing ages depends on the closing temperature of the analyzed minerals and system temperature when these minerals were formed. For example, it is obvious that $^{40}$Ar/$^{39}$Ar ages of biotites from greenschist-facies metamorphic rocks and from granites or granulite-facies metamorphic rocks should contain different geological implications. Therefore, in interpreting $^{40}$Ar/$^{39}$Ar ages, special attention should be adequately paid to the geological settings of dating samples.

### 5.1 On the age of the ductile shearing deformation events and amphibolite-facies metamorphism of UHPM rocks in central China

The age of the retrograde metamorphism of amphibolite facies of the Dabie and Sulu UHPM terranes has been an issue of hot debate. Ames et al. (1993, 1996) and Muruyama et al. (1998) argued that the ages of 210–220 Ma of zircons from UHPM rocks in the terranes represent the age of ultrahigh-pressure metamorphism. Hacker et al. (1998) believed that UHP metamorphism took place at about 240 Ma, and that the ages of 210–220 Ma of zircons records the time of retrograde metamorphism of amphibolite facies of these UHPM rocks. Structurally, the intense ductile shearing deformation event was associated with the retrograde metamorphism of amphibolite facies and responsible for the occurrence of penetrative southeast-dipping lineations and A-type folds with southeast-plunging hinges in the Donghai region. $^{40}$Ar/$^{39}$Ar dating of muscovites (Sample T98) from the Haizhou phosphorous mine gives a new constraint of the time of the amphibolite-facies metamorphism of the region, implying the occurrence of the metamorphism impossibly later than 218 Ma. At the same time, the $^{40}$Ar/$^{39}$Ar dating of the N1104-1 oriented amphiboles on the fault plane cutting the foliation and lineation of amphibolite-facies metamorphic rocks also reveals that the penetrative ductile shearing deformation and amphibolite-facies metamorphism occurred impossibly later than 213 Ma.

### 5.2 On the age of the transitional ductile-brittle deformation event and the greenschist-facies metamorphisim

It is well known that greenschist-facies metamorphism followed the amphibolite-facies metamorphism during the exhumation of UHPM rocks. But there are only a few of exact chronological data to constrain the time of the greenschist-facies metamorphism. Song et al. (1998) suggested that the metamorphism occurred in the northern Sulu region at about 155 Ma based on $^{40}$Ar/$^{39}$Ar dating of muscovites from granitic gneisses. But the present study reveals that the metamorphism and associated transitional ductile-brittle deformation event probably took place at about 213 Ma, and that the above ages of 155 Ma of muscovite, 190 Ma of K-feldspar from the Niushan gneisses and 200–204 Ma of biotites and K-feldspar from the Fangshan pegmatites are all cooling ages of these UHPM rocks and record their cooling and uplifting information. This configuration of ages getting gradually

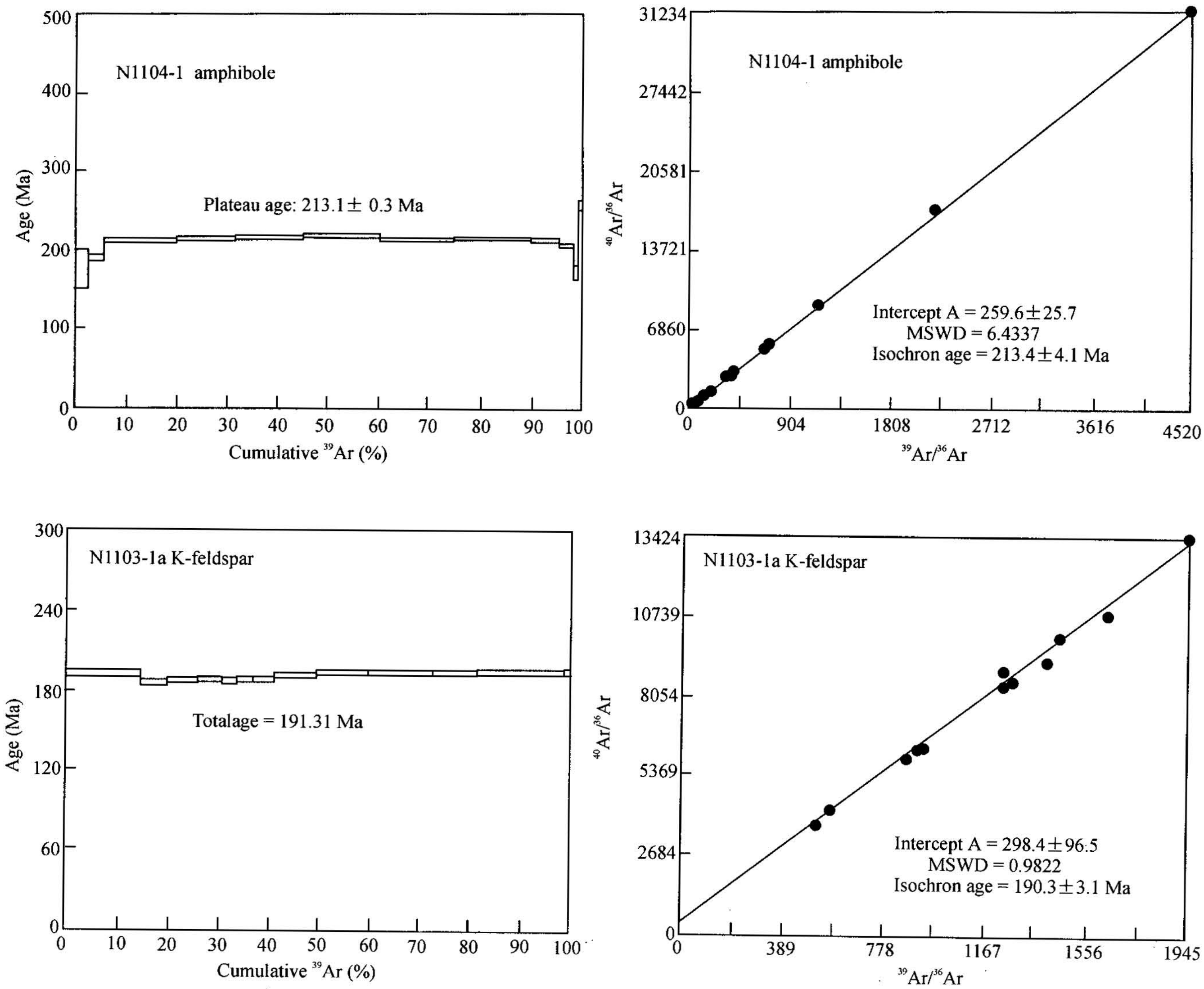


Fig. 6. $^{40}$Ar/$^{39}$Ar age plateau spectrums and isochrons of amphibolite (N1104-1) and K-feldspar (N1103-1a) from Niushan.

younger northeastwards of micas and K-feldspars is consistent with the dome-like tectonic framework with the center in the northern Sulu area, i.e., the uplifting and cooling of the southern part (Donghai region) is earlier than of northern central part, implying that the extrusion from the central part of the collisional belt resulted in the occurrence of the dome-like tectonic fromework.

### 5.3 On the exhumation processes of UHPM rocks in the Donghai region

The above comprehensive analysis indicate that the formation and exhumation of UHPM rocks in the Donghai region may be recapitulated as several events, i.e., a metamorphic event of eclogite facies at about 240 Ma (Li et al., 1993; Okay et al., 1993; Hacker et al., 1998), a ductile shearing deformation and metamorphic event of amphibolite facies at about 220 Ma, and a transitional ductile-brittle deformation and metamorphic event of greenschist facies at about 213 Ma. The exhuamtion of UHPM rocks in the Donghai region may be described as three stages as shown in Fig. 8. First stage is from the mantle of eclogite facies at about 240 Ma to the lower crust of ampnibolite facies at about 220 Ma. Providing that eclogite-facies metamorphism occurs at the depth of about 80–100 km, and the temperature of amphibolite-facies metamorphism ranges from 600–700°C, equivalent to the depth of 20–30 km (taking geothermal gradient as about 20–30°C/km), the UHPM rocks were exhumed in this stage probably at a very high rate of 3.0–4.0 km/Ma, consistent with the conclusion of a rapid exhumation suggested by petrologists. The second stage is from the lower part of the crust of amphibolite facies at 220 Ma to the middle part of

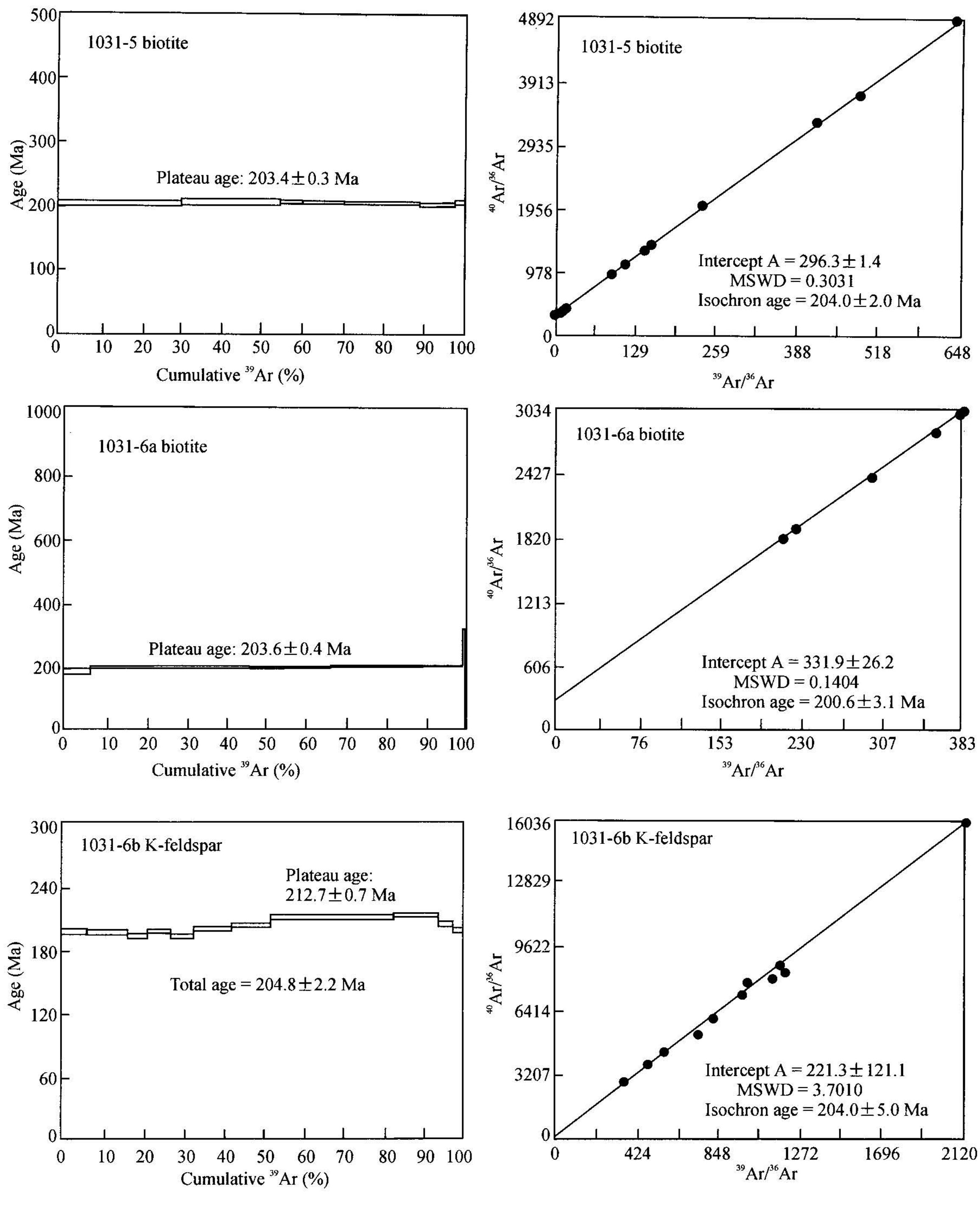


Fig. 7. $^{40}Ar/^{39}Ar$ age plateau spectrums and isochrons of biotiotes and K-feldspars from southeastern Fangshan

the crust of greenschist facies at about 213 Ma, during which the system temperature was decreased by about 100–200°C, speculating that the UHPM rocks were uplifted about 5–10 km at a rate of 1–2 km/Ma. The third stage is the elevation following the metamorphism of greenschist facies. Based on the $^{40}Ar/^{39}Ar$ dating of micas and K-feldspar, we may suppose that the UHPM rocks in Niushan of the Donghai region were exhumed from the middle part of the crust at 213 Ma to the upper part of the crust at 190 Ma at a rate of about 0.5–0.7 km/Ma, and that the UHPM rocks in Fangshan of the Donghai region were exhumed at a rate of about 1 km/Ma to the upper part of the crust at about 200 Ma. That means that UHPM rocks in Fangshan were exhumed earlier to the upper crust than those in Niushan and that the exhuming rate is gradually decreased during the exhumation of these rocks from the mantle to the

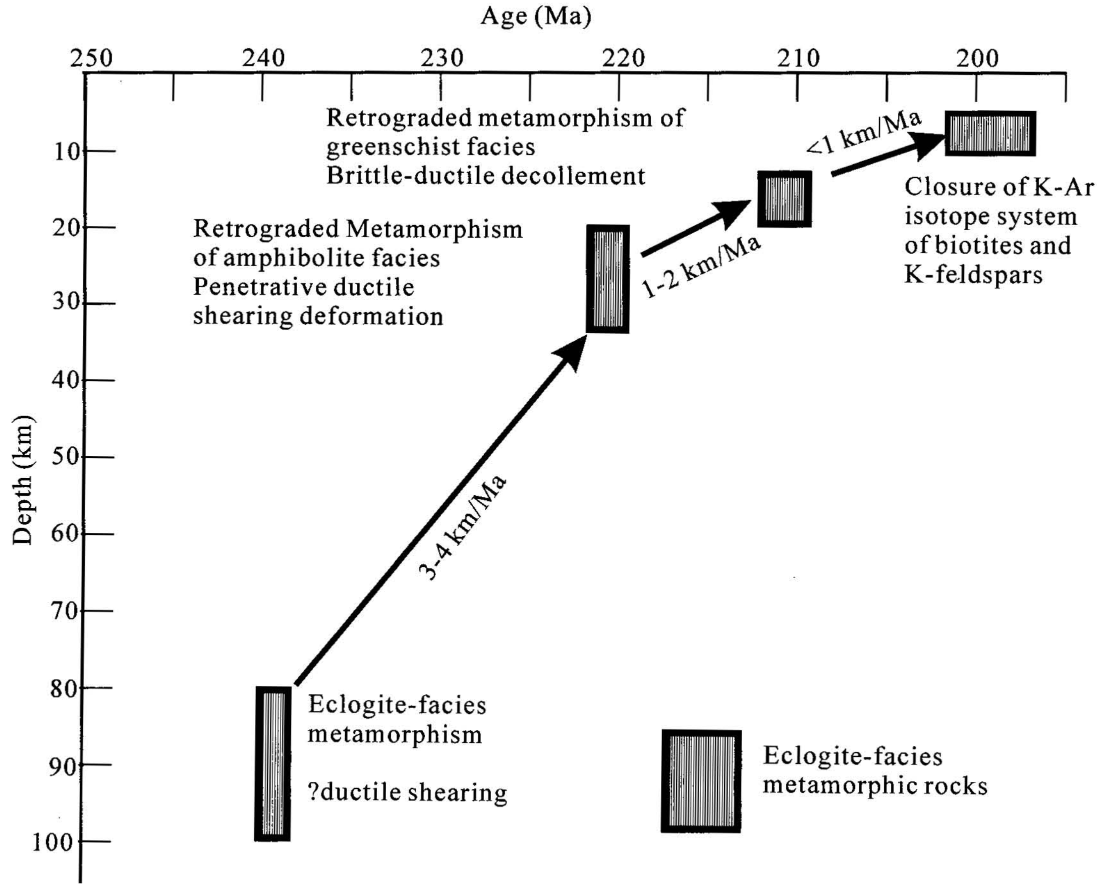


Fig. 8. Schematic diagram of exhumation of UHPM rocks in the Donghai region.

upper part of the crust.

## 6 Conclusions

Investigations into the structural deformation of UHPM rocks in the Donghai region and $^{40}Ar/^{39}Ar$ dating of amphibole, micas and K-feldspar formed in different exhuming stages imply that ductile and transitional ductile-brittle deformation events during the exhumation of these rocks are in turn associated with metamorphic phases of amphibolite facies and greenschist facies, and took place at 220 Ma and 213 Ma, respectively. And then, the exhumation of these rocks from 240 Ma to 190 Ma is briefly reconstructed based mainly on the thermal chronological data. It is to be pointed out that the reconstruction of the exhumation of the UHPM rocks is initial and open to revisions due to the lack of detailed data on the cooling history of the rocks.

## Acknowledgements

This study was financially supported by the former Ministry of Geology and Mineral Resources of China (grant No. 9501102). We specially appreciate Prof. Wang Yu for his help in $^{40}Ar/^{39}Ar$ dating of some samples and his constructive suggestions in preparation of this paper.

Manuscript received Feb. 22, 2002
accepted Feb. 11, 2003
edited by Hao Ziguo and Xie Guanglian

### References

Ames, L., Tilton, G. R., and Zhou, G. Z., 1993. Timing of collision of the Sino-Korean and Yangtze cratons: U-Pb zircon dating of coesite-bearing eclogites. *Geology*, 21: 339–342.

Ames, L., Zhou, G., and Xiong, B., 1996. Geochronology and isotopic character of ultrahigh-pressure metamorphism with implications for collision of the Sino-Korean and Yangtze cratons, central China. *Tectonics*, 15(2): 472–489.

Chen Wenji, Harrison, T. M., Heizler, M. T., LIU Ruoxin, MA Baolin and LI Jiliang, 1992. The cooling history of melange zone in North Jiangsu-South Shandong-South Shandong region: evidence fron multiple diffusion domain $^{40}Ar$-$^{39}Ar$ thermal geochronoly. *Acta Petrologica Sinica*, 8(1): 1–17 (in Chinese with Eanglish abstract).

Cheng Yuqi, Liu Dunyi, Williams, I. S., Jian Ping, Zhuang Yuxun and Gao Tianshan, 2000. SHRIMP U-Pb dating of zircons of a dark eclogite and a garnet-bearing gneissic granitic rock from the Dabie Mountains, Luotian county, Hubei province, China:

New evidence for early Precambrian evolution. *Acta Geologica Sinica* (English edition), 74(4): 748–765.

Cong Bolin. 1996. *Ultrahigh-pressure Metamorphic Rocks in the Dabieshan-Sulu Region of China*. Beijing: Science Press and London: Kluwer Academic Publishers, 224.

Cong, B., Wang, Q., Zhai, M., Zhang, R. Y., Zhao, Z., and Ye, K. 1994. UHP metamorphic rocks in the Dabie-Su-Lu region, China: their formation and exhumation. *The Island Arc*, 3:135–150.

Dodson, M. H., 1973. Closure temperature in cooling geochronological and petrological systems. *Contrib. Mineral. Petrol.*, 40:259–274.

Dong Shuwen, Wu Hongling, Liu Xiaochun and Xue Huaimin, 2002. On continent-continent point-collision and ultrahigh-pressure metamorphism. *Acta Geologica Sinica* (English edition), 76(1): 69–80.

Enami, M. and Zhang, Q., 1990. Quartz pseudomorphs after coesite in eclogites from Shandong province, east China. *American Mineralogist*, 75: 381–386.

Ernst, W. G., Liou, J. G., Hacker, B. R., 1994. Petrotectonic significance of high- and ultrahigh-pressure metamorphic belts: inference for subduction-zone histories. *International Geology Review*, 36: 213–237.

Fu Yunlian, Luo Xiuquan, Zhang Sihong and Wang Lutong, 1987. $^{40}Ar/^{39}Ar$ dating techniques and age determination of some geological samples. *Bulletin of the Institute of Geology, Chinese Academy of Geological Sciences*, (17): 85–107 (in Chinese with English abstract).

Hacker, B. R., Ratschbacher, L., Webb, L., Ireland, T., Walker, D., and Dong Shuwen. 1998. U/Pb zircon ages constrain the architecture of the ultrahigh-pressure Qinling-Dabie Orogen, China. *Earth and Planetary Science Letters*, 161: 215– 230.

Hacker, B. R., Ratschbacher, L., Webb, L.E., Dong, S.,1995. What brought them up? Exhumation of the Dabie Shan ultrahigh-pressure rocks. *Geology*, 23(8): 743–746.

Hirajima, T., Ishiwatari, A., Cong, B. L., Zhang, R. Y., Banno, S., and Nozaka, T., 1990. Coesite from Mengzhong eclogite from Donghai country, northeastern Jiangsu province, China. *Mineralogical Magazine*, 54: 579–583.

Hu Shouxi, Sun Jinggui, Ling Hongfei, Ye Ying, Fang Changquan and Zhaoyiying. 2001. The Lanshantou kyanite-bearing eclogite with coesite inclusions in the Sulu ultrahigh-pressure metamorphic belt and its PTt path. *Acta Geologica Sinica* (English edition), 75(4): 409–420.

Jian Ping, Liu Dunyi, Yang Weiran, and Williams, I. S., 2000. Petrographic and SHRIMP studies of zircons from the Caledonian Xiongdian eclogite, Northwestern Dabie Mountains. *Acta Geologica Sinica* (English edition), 74(4): 766–773.

Lee, Y. S., Nishimura, S., and Min, K. D., 1997. Paleomagnetotectonics of East Asia in the Proto-Tethys Ocean. *Tectonophysics*, 270:157–166.

Li Jinyi, 2001. Pattern and time of the collision between thr Sino-Korean and Yangtze blocks: evolution of the Sinian-Jurassic sedimentary settings in the Middle-lower reaches of the Yangtze rive. *Acta Geologica Sinica* (Chinese edition). 75(1): 25–34 (in Chinese with English abstract).

Li Qi, Chen Wenji, Ma Baolin, Wang Qingchen and Sun Min, 1995. Thermal evolution history after collision of North China plate with Yangtze plate. *Seismology and Geology*, 17(3): 193–203 (in Chinese with English abstract).

Li Shuguang, Xiao Yilin, Liu Deliang, Chen Yizhi, Ge Ningjie, Zhang Zongqing, Sun Shen-su, Cong Bolin, Zhang Ruyuan, Hart, S. R., and Wang Songshan. 1993. Collision of the North China and Yangtze blocks and formation of coesite-bearing eclogites, timing and processes. *Chemical Geology*, 109: 89–111.

Li Zheng-Xiang. 1994. Collision between the north and South China blocks: A crustal-detachment model for suturing in the region east of the Tanlu foult. *Geology*, 22: 739–742.

Liou, J. G. and Zhang, R. Y., 1996. Occurrence of intergranular coesite in Sulu ultrahigh-P rocks from China: Implications for fluid activity during exhumation. *Am. Mineral.*, 81: 1217–1221.

Liou, J. G., Zhang, R. Y., Edie, E. A., Maruyama, S., and Ernst, W. G., 1996. Metamorphism and tectonics of high-P and ultrahigh-P belts in the Dabie-Su-Lu region, eastern Central China. In: Harrison, T. M. and Yin, A. (eds.), *The Tectonics of Asia*, Rubey Volume VIII. Englewood Cliffs, New Jersey: Prentice-Hall, Inc., 300–344.

Lister, G. S. and Baldwin, S. L., 1996. Modeling the effect of arbitrary *P-T-t* histories on argon diffusion in minerals using the MacArgon program for the Apple Macintosh. *Tectonophysics*, 253:83–109.

Liu Fulai, Xu Zhiqin, Xu Huifen and Yang Jingsui, 1999. High and ultrahigh-pressure metamorphism and retrogressive texture of gneiss in the Donghai area—evidence from gneisses in drillhole ZK2304. *Acta Geologica Sinica* (English edition), 73 (3): 300-315

Liu Fulai, Zhang Zeming, Xu Zhiqin, Yang Jingsui and Xu Huifen, 2000. Micro-area chemical composition and preserved P-T evolution trace of phengite in albite gneiss from the Donghai ultrahigh-pressure metamorphic area, East China. *Acta Geologica Sinica* (English edition), 74(2): 182-189

Maruyama, S., Liou, J. G., and Zhang, R., 1994. Tectonic evolution of the ultrahigh-pressure and high-pressure metamorphic belts from central China. *The Island Arc*, 3: 112–121.

Maruyama, S., Tabata, H., Nutman, A. B., Morikawa, T., and Liou, J. G., 1998. SHRIMP U-Pb geochronology of ultrahigh-pressure metamorphic rocks of the Dabie mountains, central China. *Continental Dynamics*, 3(2): 72–85.

Masaki, E., Quija Zang and Yujun Yin. 1993. High-pressure eclogites in northern Jiangsu-southern Shandong provinces, eastern China. *J. Metamorphic Geol.*, 11:589–603.

McGrew, A. J., and Snee, L. W., 1994. $^{40}Ar/^{39}Ar$ thermochronologic constraints on the tectonothermal evolution of the northern East Humboldt Range metamorphic core complex, Nevada. *Tectonophysics*, 238: 425–450.

Meng Qinren, and Zhang Guowei, 1999. Timing of collision of the North and South China blocks: Controversy and reconciliation. *Geology*, 27(2): 123–126.

Okay, A. I., Sengor, A. M. C., and Satir, M., 1993. Tectonics of an ultrahigh-pressure metamorphic terrane: the Dabie Shan/ Tongbai Shan orogen, China. *Tectonics*, 12: 1320–1334.

Okay, A. I., Xu, S. and Sengor, A. M. C., 1989. Coesite from Dabie Shan eclogites, central China. *European Journal of Mineralogy*, 1: 595–598.

Platt, J. P., 1993. Exhumation of high-pressure rocks: a review of concepts and processes. *Terra Review*, 5: 119–133.

Song Mingchun and Lu Fatang, 1998. Primary study on muscovite from the country rock of eclogites in Jiaonan area, Shandong province. Journal of Mineralogy and Petrology, 17 (2): 17–21 (in Chinese with English abstract).

Wallis, S. R., Ishiwatari, A., Hirajima, T., Ye, K., Guo, J., Nakamura, D., Kato, T., Zhai, M., Eami, M., Cong, B., and Banno, S., 1997. Occurrence and field relationships of ultrahigh-pressure metagranitoid and coesite eclogite in the Su-Lu terrane, eastern China. *Journal of the Geological Society*, London, 154: 45–54.

Wang Qingchen, Zhang Ruyuan, Cong Bolin, Zhao Zhongyan and Ye Kai. 1992. Eclogites in eastern Shandong-northern Jiangsu region: their structure and exhumation mechanism. *Acta Petrologica Sinica*, 8(2):153–160 (in Chinese with English abstract).

Wang, X., and Liou, J. G., 1992. Regional ultrahigh-pressure coesite-bearing eclogitic terrane in central China: evidence from country rocks, gneiss, marble, and metapelite. *Geology*, 19: 933–936.

Xu Shutong, Okay, A. I., Ji Shouyuan, Sengor, A. M. C., Su Wen, Liu Yican and Jiang Laili, 1992. Diamonds from Dabie Shan metamorphic rocks and its implication for tectonic setting. *Science*, 256: 80–82.

Xu, Z. Q., 1987. Étude Tectonique et Microtectonique de là Chine Paléozoïque et Triasique de Qinling. *Présente to L'Université des Sciences et Techniques dû Languedoc pour obtenir le diplômé de Doctorat*. 93–107.

Yang Jianjun, Godard, G., Kienast, J.-R., Lu, Y, and Sun, J., 1993. Ultrahigh-pressure (60km) magnesite-bearing garnet peridotites from northeastern Jiangsu, China. *The Journal of Geology*, 101:541–554.

Yang Tiannan, Xu Huifen, Zhang Jianxin, and Zeng Lingsen, 1996. Deformation history of Jiaonan UHP terrane. *Continental Dynamics*, 1(2): 164–170.

Yin, A., and Nie, S., 1993. An indentation model for the North and South China collision and the development of the Tan-Lu and Honam fault system, eastern Asia. *Tectonics*, 12: 801–813.

Zhang Guowei, Meng Qingren and Lai Shaocong, 1995. Tectonics and structure of Qinling orogenic belt. *Science in China (B)*, 38(11): 1379–1394.

Zhang Ru-Yuan, Hirajima, T., Banno, S., Cong, B., and Liou, J. G., 1995. Petrology of ultrahigh-pressure rocks from the southern Su-Lu region, eastern China. *J. Metamorphic Geol.*, 13: 659–675.

Zhang, R., Hirajima, T., Banno, S., Ishiwatari, A., Jiaju Li, Cong, B., and Nozaka, T., 1990. Coesite-eclogite from Donghai area, Jiangsu province in China. In: The 15th General Meeting of the International Mineralogical Association Abstracts, 2: 923–924.

Zhu Guang, Xu Jiawei, Liu Guosheng, Li Shuangying, and Yu Peiyu. 1999. Tectonic pattern and dynamic mechanism of the foreland deformation in the lower Yangtze region. *Regional Geology of China*, 18(1): 73–79 (in Chinese with English abstract).